Chapter-5

Synthesis and characterization of Mg20Zn2Mn based composite reinforced with HAp and S45P7 BAG

5.1 Introduction

The present chapter describes the synthesis and characterization of $MgZn_{20}Mn_2$ based composites added with different amounts of HAp and S45P7 BAG. The detailed method adopted for the preparation of the alloy, HAp and S45P7 BAG has been explained in the previous chapter (chapter 4, section 4.2). A brief synthesis process can be understood from the below mentioned flow chart in Fig. 5.1.

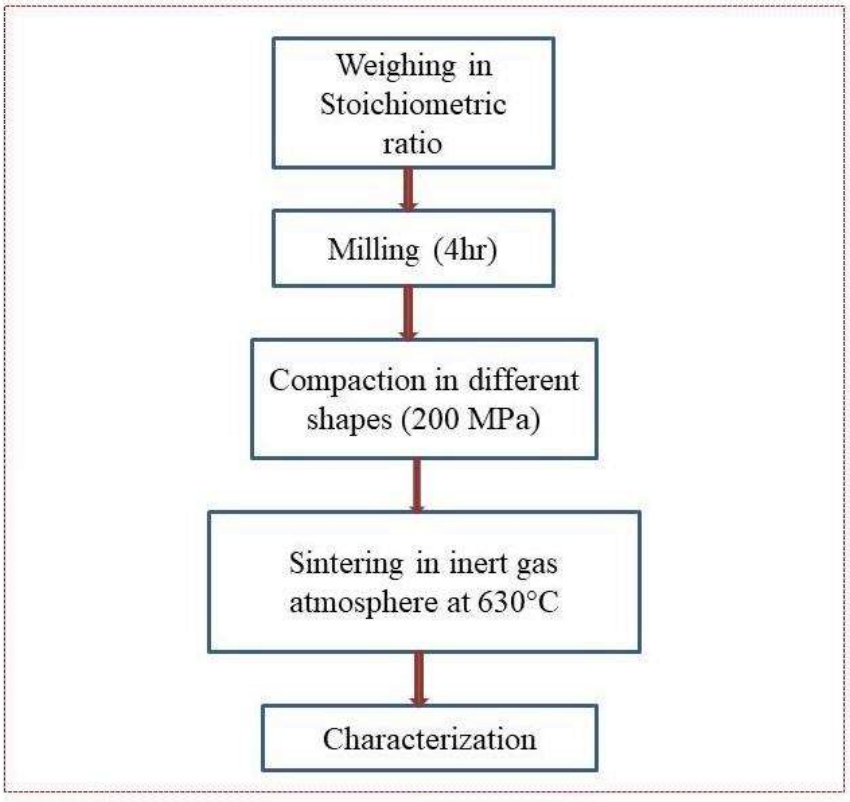

FIGURE 5.1: Flow diagram of preparation of composite specimens

The prepared specimens were then characterized and their mechanical properties viz. hardness, young's modulus, flexural strength, and compressive strength were examined. To get the microstructural examination and surface characterization SEM and XRD tests were performed. The characteristics of the chemical bond formed by the composites after immersion in SBF were detected by FTIR analysis. With the help of FTIR different corrosion layers formed on the surface can be determined.

5.2 Preparation of Composites

The magnesium alloy was prepared with the addition of 20 % Zn and 2%Mn in magnesium as discussed in chapter 3, section 3.4. The prepared alloy was then reinforced with HAp and S45P7 BAG in different proportions as mentioned in Table 5.1.

Table 5.1: Alloy-reinforcement proportions

S.N	Base Alloy	HAp (wt %)	S45P7 BAG (wt %)
1.	Mg20Zn2Mn	5	-
2.	Mg20Zn2Mn	10	-
3.	Mg20Zn2Mn	20	-
4.	Mg20Zn2Mn	-	5
5.	Mg20Zn2Mn	-	10
6.	Mg20Zn2Mn	-	20
7.	Mg20Zn2Mn	2.5	2.5
8.	Mg20Zn2Mn	5	5
9.	Mg20Zn2Mn	10	10

5.3 Results and Discussion

5.3.1 X-ray Diffraction (XRD)

The XRD of all the composite specimens and base alloy before and after the shows the phases formed. The standard XRD peak for pure Zn crystal and pure Mg crystal has been shown in Fig. 5.2 and Fig. 5.3, respectively.

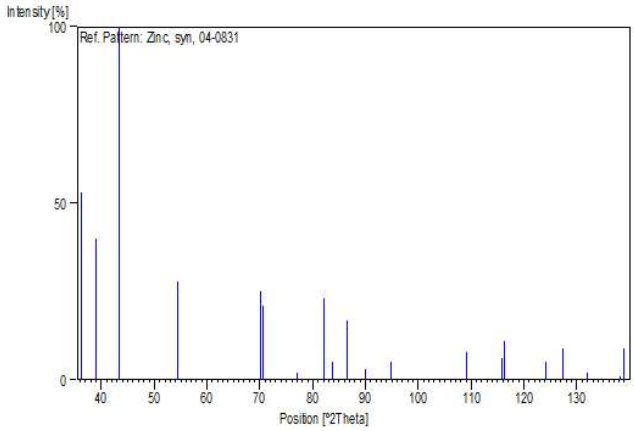

FIGURE 5.2: Reference peak for zinc crystal

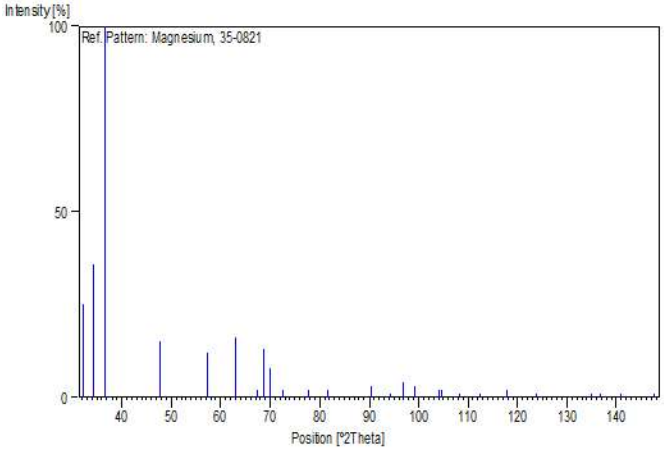

FIGURE 5.3: Reference peak for magnesium crystal

The peaks of pure metals has standard reference peak as shown above. The JCPDS number corresponding to zinc metal is JCPDS: 04-0831 and the standard value for magnesium is observed at JCPDS: 35-0821.

The XRD pattern of the base alloy, alloy-bioactive glass composites, alloy-HAp composites and alloy-bioactive glass-HAp for both unfired and fired composites (i.e. after sintering) are shown in Fig 5.4, 5.5, 5.6, 5.7, 5.8 and 5.10 respectively. The XRD patterns of all the above compositions show crystalline phases of Magnesium [M, card number: JCPDF# 895003)], Zinc [Z, card number: JCPDF# 657219], while for HAp and the alloy-HAp composites shows the crystalline phases of β-TCP [$Ca_3(PO_4)_2$, card number: JCPDF# 700364] and Hydroxyapatite and Calcium ammonium phosphate hydrate [$CaNH_4PO_4(H_2O)_7$, card number: JCPDF# 750703]. XRD patterns specifically for fired sample show a particular phase of Magnesium-Zinc [MZ, card number JCPDF# 654290].

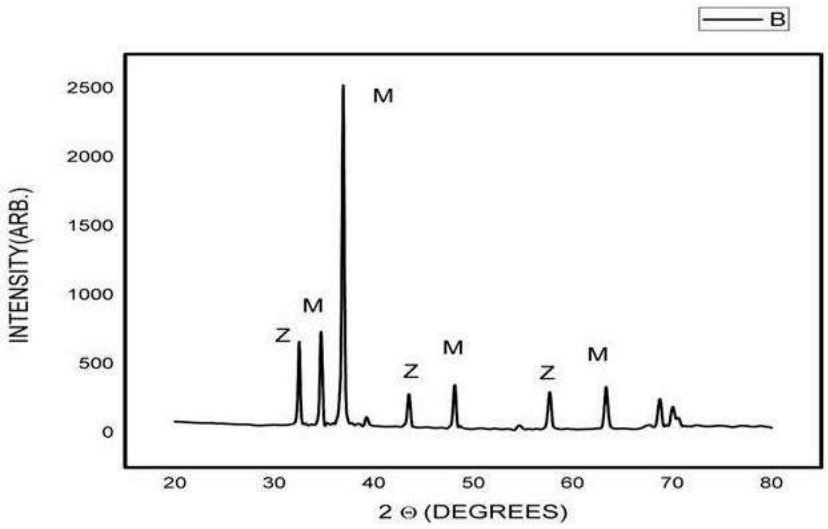

FIGURE 5.4: XRD peak of unfired base alloy (Mg20Zn2Mn)

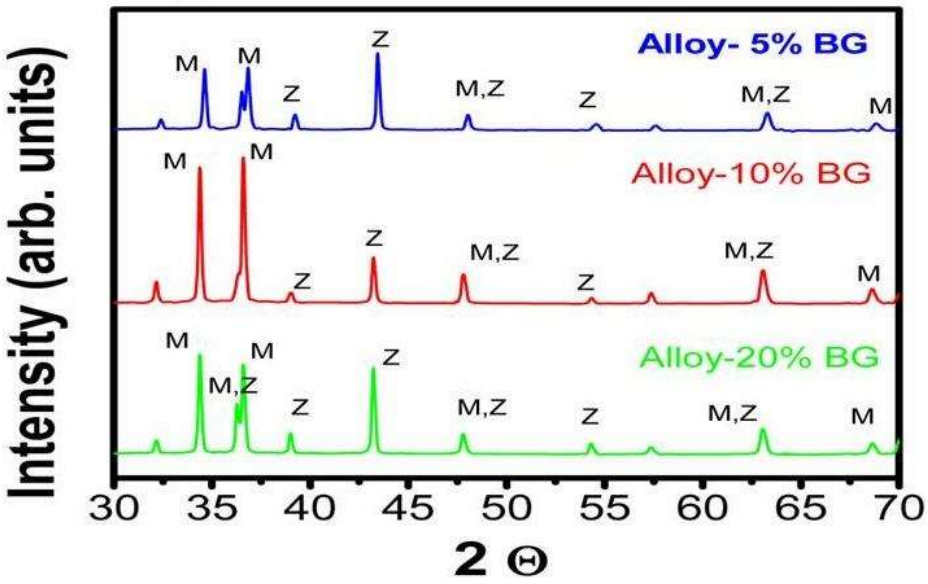

FIGURE 5.5: XRD patterns of unfired alloy-bioactive glass composite in various proportions

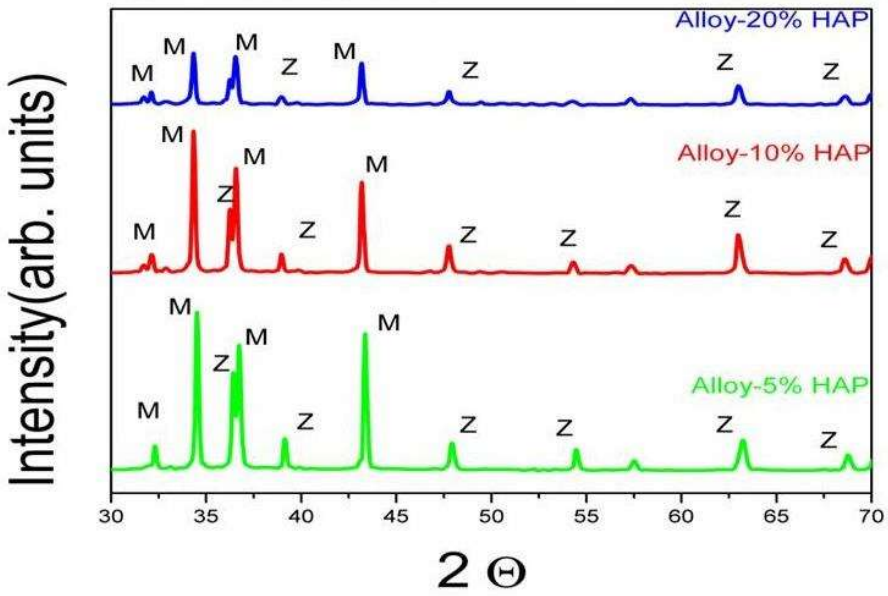

FIGURE 5.6: XRD patterns for unfired alloy-HAp composite in various proportions

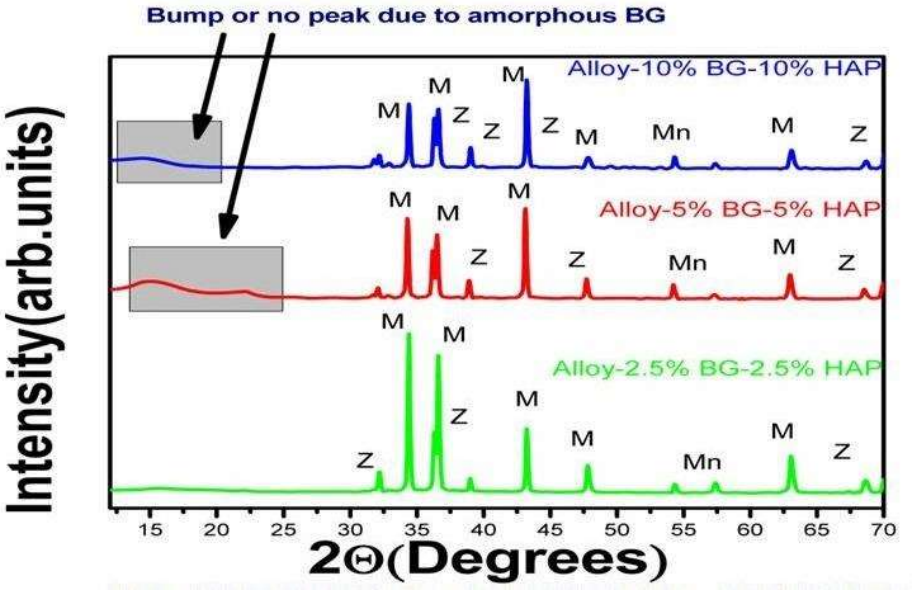

FIGURE 5.7: XRD patterns of unfired Alloy-HAp-bioactive glass composites

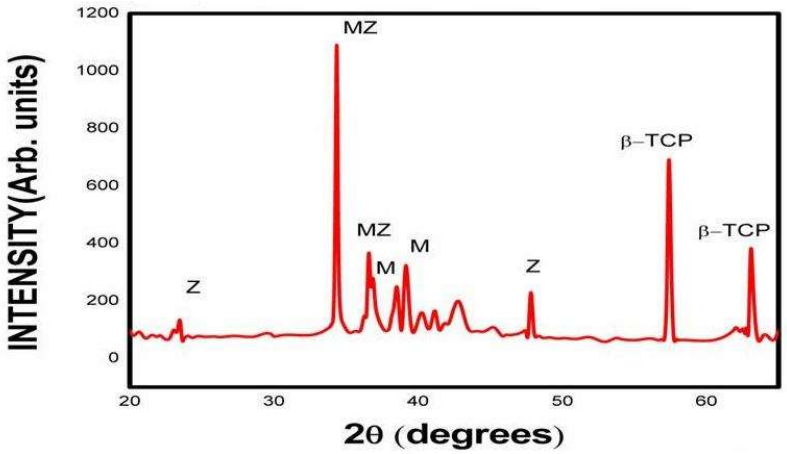

FIGURE 5.8: XRD patterns for fired Alloy-HAp composite

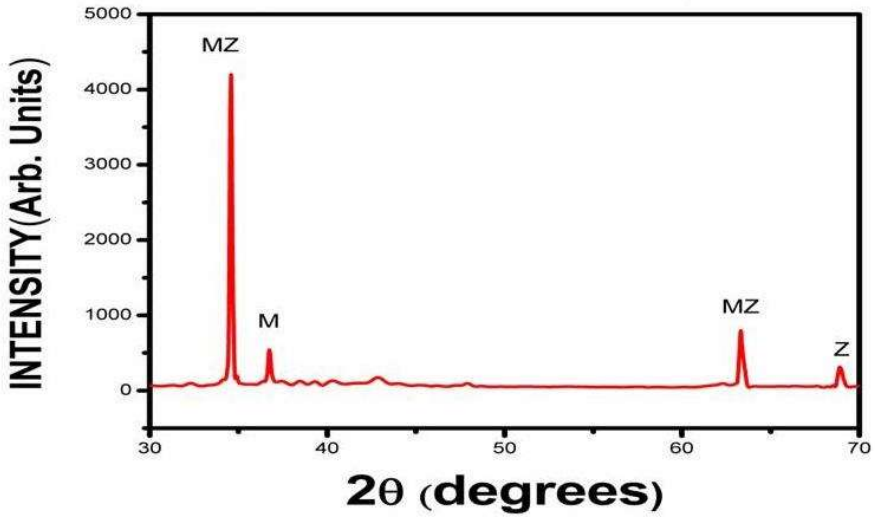

FIGURE 5.9: XRD patterns for fired Alloy- bioactive glass composite

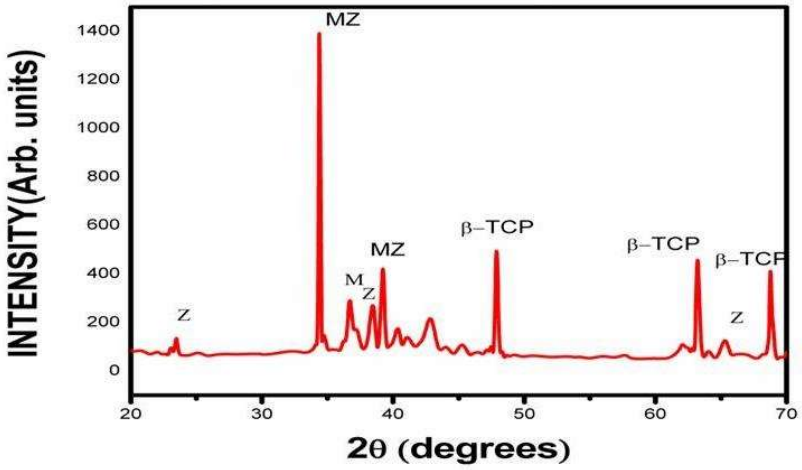

FIGURE 5.10: XRD patterns for fired Alloy-HAp-bioactive glass composite

The XRD pattern of the alloy-composites prepared before and after sintering has shown the phases formed and proper sintering of the composite. The XRD patterns for alloy, HAp, alloy–bio-active glass composites, alloy–HAp composites and alloy–bio-active glass–HAp were observed for unfired and fired samples. The XRD patterns of all the above compositions show crystalline phases of magnesium, zinc, while for HAp and the

alloy–HAp composites the crystalline phases of β-tricalcium phosphate (TCP), HAp and calcium ammonium phosphate hydrate were observed. The phases detected before and after firing is mentioned in Table no. 5.2

TABLE 5.2: Phases detected in fired and unfired samples

S.N	Base Alloy	Reinforcement	Phases detected	
			Unfired Samples	Fired Samples
1.	Mg20Zn2Mn	Nil	Magnesium (M), Zinc (Z)	M, Z, MZ
2.	Mg20Zn2Mn	HAp	Magnesium (M), Zinc (Z)	MZ, M,Z, β-TCP
3.	Mg20Zn2Mn	S45P7 BAG	Magnesium (M), Zinc (Z)	MZ, Z, M,
4.	Mg20Zn2Mn	HAp + S45P7 BAG	Magnesium (M), Zinc (Z), Manganese (Mn)	M, Z, MZ, β-TCP

5.3.2 Microstructure Evolution

Figure 5.11 to 5.14 shows the various SEM images of the fired samples at different magnifications.

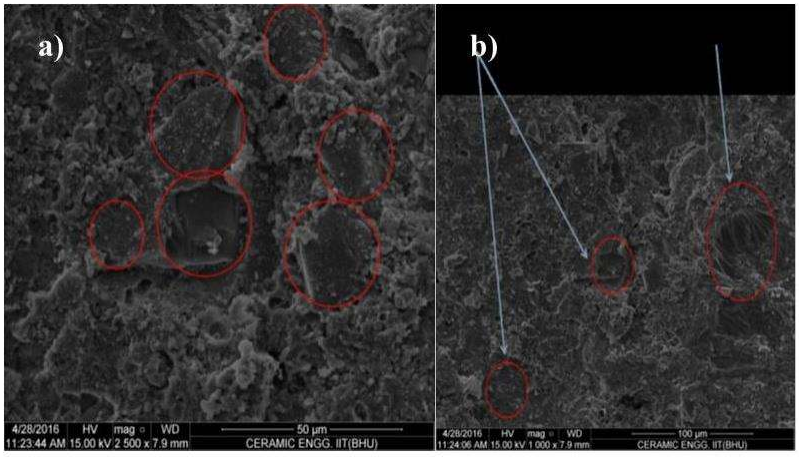

FIGURE: 5.11 SEM image of sample containing HAp

Figure 5.11(a) shows the SEM image of sample 1 (i.e., Alloy-5 % HAp), specific areas showing regions of high grade densities. Figure 5.11 (b) specifically shows a region where ridges are formed like a waterfall, shows the melting of various constituents in the sample (viz., Zinc, B2O3, P2O5 etc.) leading to a conclusion that the sample is trying to reduce its porosity.

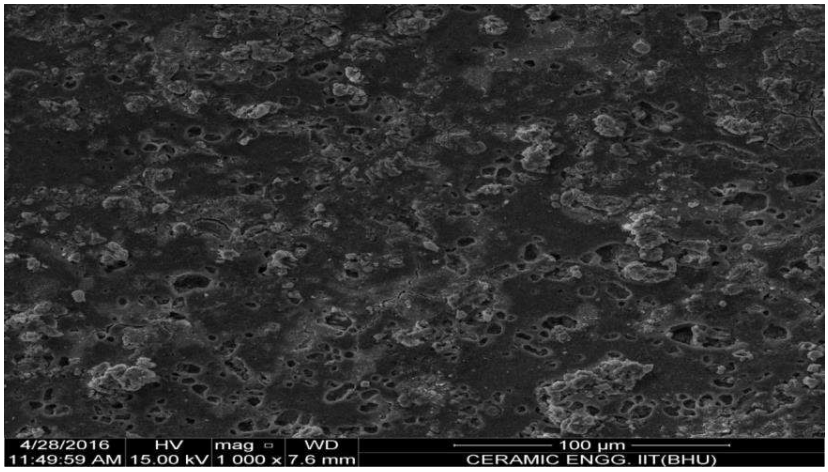

FIGURE 5.12 (a) SEM images of composite with 10% HAp showing evolution of gases

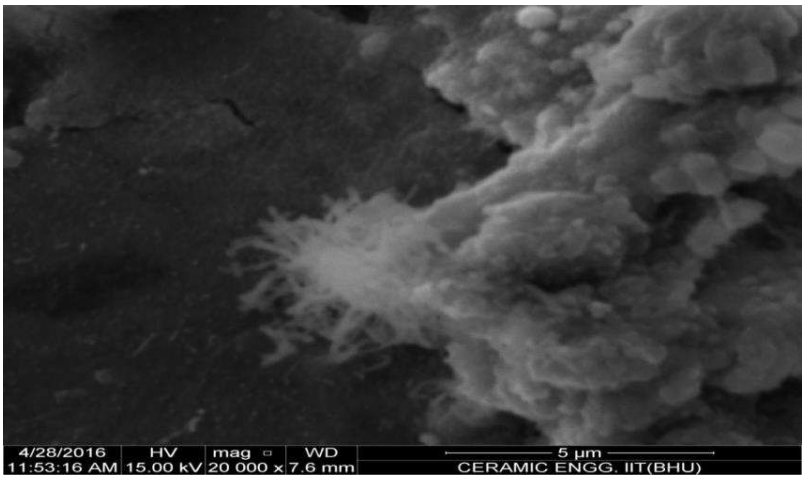

FIGURE 5.12 (b) Shows HAp flakes on the surface of the sample

Further, Fig. 5.12 (a) suggests that a lot of volatile gases and water of hydration has evolved out of the sample attributed to numerous pockets showing up on the surface of the sample. Fig. 5.12 (b) suggests that HAp has come up over the surface of the sample as seen like flowering object on the surface of the sample.

Fig. 5.13 suggests that the whitish surface is either due to S45P7 BAG, because of the different absorption, transmittance, reflectance capacities of the constituent particles for the electron bombardment in the sample or it might be due to variations in the absorption, transmittance, and reflectance capacities of the sample as a whole.

FIGURE 5.13 SEM image of sample containing S45P7 BAG

Fig. 5.14 (a, b) shows a lot of even flowering on the surface of the sample which is either due to 45S5P7 BAG, or due to β-TCP on the surface, thus leading to a results that the

sample will show high bioactivity towards in-vivo experiments also it will show high osteo- conductivity for the bones

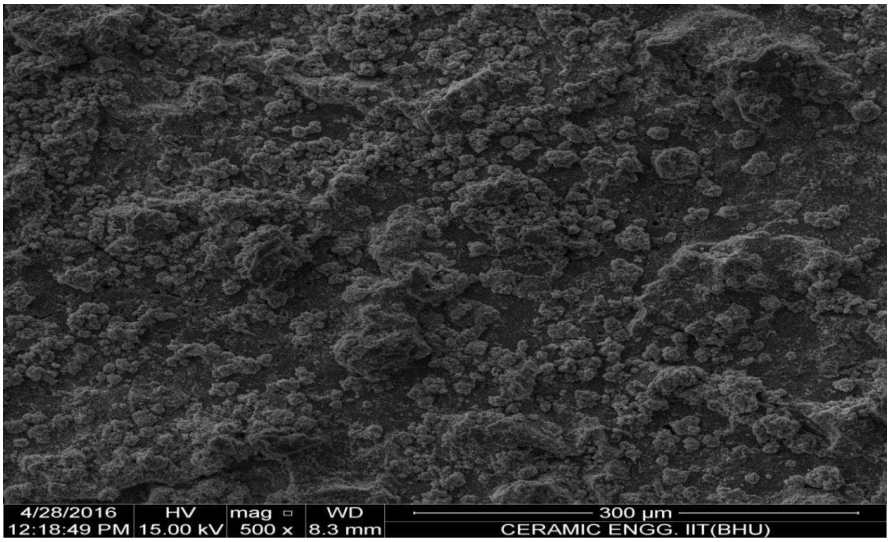

FIGURE 5.14 (a) SEM images of sample with 5 % HAp and 5 % S45P7 BAG spread over whole crystals

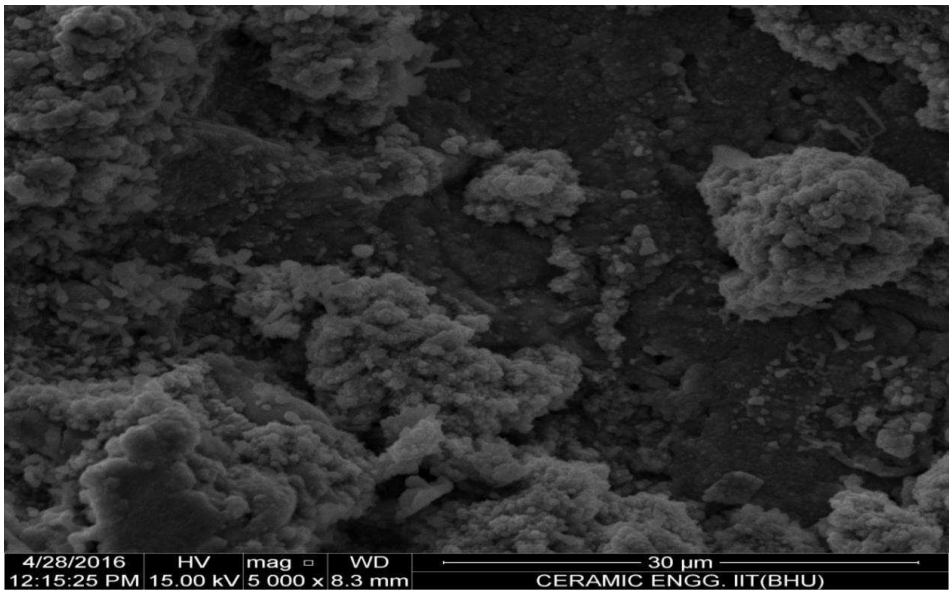

FIGURE 5.14 (b) SEM images of sample with 10 % HAp and 10% S45P7 BAG

5.3.3 Fourier Transform Infrared Spectroscopy

The Fourier transform infrared (FTIR) reflectance spectra of bioactive glasses, Alloy-HAp, Alloy-45S5P7 BAG and Alloy-45S5P7 BAG-Hap composites, and HAp are given in Figures 5.15-5.17.

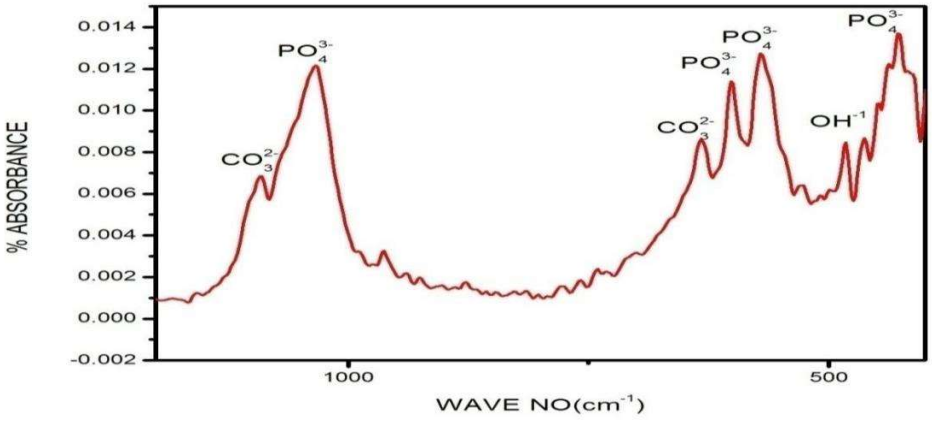

FIGURE 5.15 FTIR spectrum of HAp

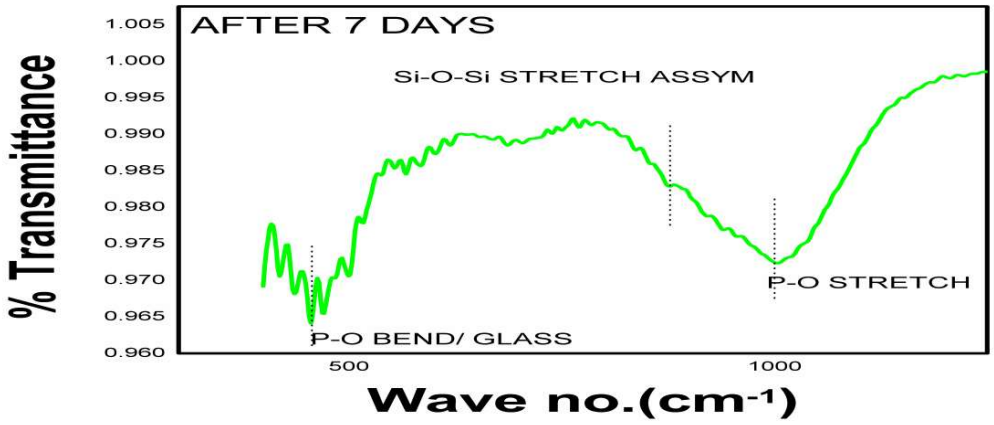

FIGURE 5.16 FTIR spectrum of S45P7 bioactive glass when kept in SBF solution for 7 days

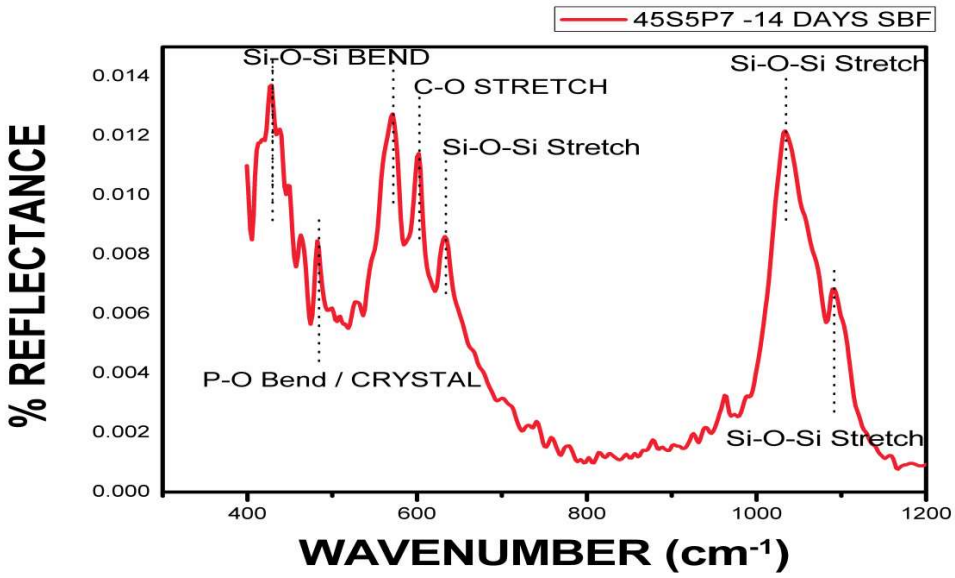

FIGURE 5.17 FTIR spectrum of S45P7 bioactive glass when kept in SBF solution for 14 days

Following changes were observed in the FTIR reflectance spectra of bioactive glass S45P7 at various reaction times. After soaking for 1 day in SBF solution peak at wavenumber 471cm^{-1} shifted to lower wavenumber at 461 cm^{-1} and peak at wave number 1100 cm^{-1} shifted to higher wavenumber at 1125 cm^{-1} with decreasing their intensity, while the peak at wavenumber 930 cm^{-1} had disappeared. Appearance of new peaks at wavenumbers 557, 607, 794, 871, 1050, and 1250 cm^{-1} were observed. After 3 days, intensity of peaks at wave numbers 557, 794, 1125, 1250 cm^{-1} decreased while the intensity of peaks at wavenumbers 607, 871, 1050 cm^{-1} increased. After 7 days peak at wave number 471 cm^{-1} which was found earlier disappeared. Appearance of peak at wavenumbers 527 cm^{-1} was observed. After 15 days, peaks at wavenumbers 527, 607, 871, 1050 cm^{-1} were dominant in the FTIR reflectance spectra. Careful inspection of FTIR reflectance spectra of all the metal-ceramic composites (2, 5, 7, and 9) in comparison with

the base bioactive glass (S45P7) reveals minor or limited variation of the positions and intensities of the reflectance peaks. The main differences can be summarized in Alloy-45S5P7 BAG-HAp, where there was time delay in the formation of peaks at wavenumbers 527 and 607 cm^{-1}. Fig. 5.18 shows the FTIR spectrum of composite samples with reinforcement of 45S5P7 BAG and Hap in different proportions.

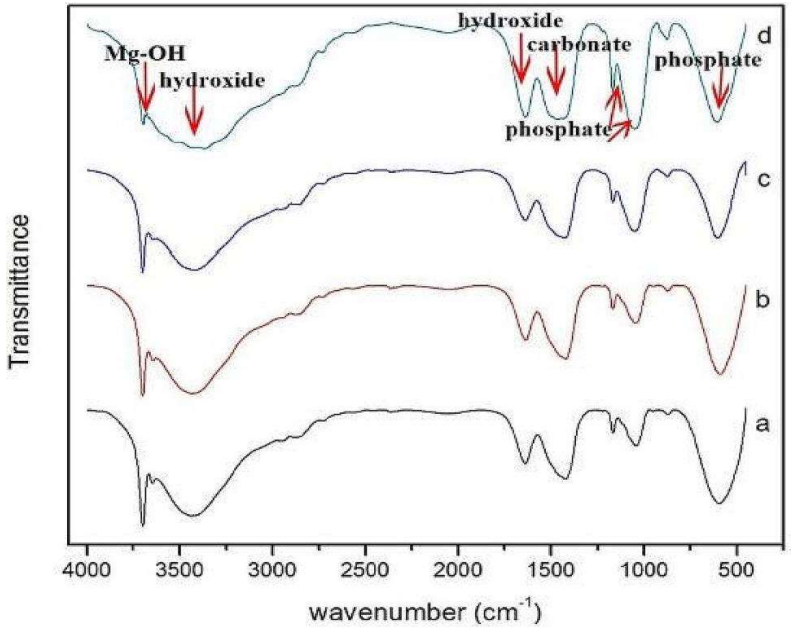

FIGURE 5.18: FTIR spectrum of composite samples with reinforcement of (a) 10 wt% HAp, (b) 10 wt% bio-glass, (c) 5 wt% each of HAp and bio-glass and (d) 10 wt% HAp + 10 wt% bio-glass after 14 days of immersion in SBF

From FTIR data of the composites with different percentages of HAp and S45P7 BAG it was found that after the immersion in SBF for 14 days, there are three major groups present in the spectrum: OH^-, PO_4^{3-} and CO_3^{2-}. Bands in the range of 630–573 cm^{-1} are attributed to phosphate amorphous band, while the bands at 1043 and 1165 cm^{-1} are caused by stretching mode vibration of PO_4^{3-} and CO_3^{2-}. Stretching mode vibration can

also be observed at about 1420 cm^{-1}. The broad bands at 3437 and 1637 cm^{-1} are assigned to OH stretching and bending, respectively. This broad band mainly comes from water due to the strong H bonding inside the structure. A sharp peak at about 3644 cm^{-1} indicates the presence of $Mg(OH)_2$, which is the corrosion product from magnesium matrix. The carbonate and phosphate bands are observed to be more broad and deep with the increase of weight percentage of bioactive glass. This shows that more CO_3^{2-} and PO_4^{3-} group are coupled in the apatite. More bioactive glass composition in the composites will lead to more migration of Ca^{2+} and PO_4^{3-} groups from the solution to composites surface. This is because of the condensation and polymerization of SiO_2 rich layer on the sample surface. SiO_2 rich layer will stimulate the migration of Ca^{2+} and PO_4^{3-} (M.R. Majhi, et al. 2015). This is due the precipitation of ions from the solution itself. It can be seen from the shallow peak of carbonate, hydroxide and phosphate. From all of the element groups observed through FTIR spectrum, it can be concluded that immersion of Mg-Zn-Mn alloy, Alloy-S45P7 BAG , Alloy-HAp-BAG composites in SBF solution will stimulate the formation of carbonated apatite on the sample surface. These products formed on the surface of the composites acts as a protective layer and prevent the further degradation of materials in the corrosive media.

5.3.4 Mechanical characteristics

The mechanical characteristics of the magnesium alloy based composites were measured by the procedure discussed in section 4.6. The value of mechanical characteristics is mentioned in Table 5.3.

TABLE 5.3: Mechanical properties of different composites

S.N	Reinforcement (%)	Hardness (HV)	Young's Modulus (GPa)	Flexural Strength (MPa)	Compressive Strength (MPa)
1.	5HAp	112.14 ± 1.14	46.5 ± 2.14	114.43 ± 3.14	123.44 ± 2.56
2.	10HAp	117.47 ± 2.73	46.8 ± 1.24	119.92 ± 2.78	127.12 ± 3.19
3.	20HAp	114.71 ±1.87	45.3 ± 3.14	115.22 ± 1.79	119.88 ± 3.12
4.	5BAG	113.46 ± 1.69	44.8 ± 2.16	112.74 ± 2.88	121.49 ± 2.88
5.	10BAG	116.23 ± 1.86	38.2 ± 1.86	117.28 ± 3.65	126.40 ± 2.98
6.	20BAG	112.95 ± 2.11	36.6 ± 2.31	115.36 ± 2.34	122.21 ± 3.88
7.	2.5HAp+ 2.5 BAG	112.33 ± 2.43	43.9 ±1.98	112.51 ± 3.91	123.65 ± 2.93
8.	5HAp+ 5 BAG	117.12± 1.98	37.8 ± 2.78	118.15 ± 1.67	129.12 ± 3.16
9.	10HAp+ 10 BAG	110.27 ± 1.98	36.1 ± 1.43	114.67 ± 3.22	121.47 ± 2.33

The mechanical strength of the composites greatly depends upon the extent of densification, proper sintering and minimum pores present in the composites. It was observed from the mechanical tests that the composite with 10 % reinforcement has better properties than that of 5 % or 20 % reinforcement. This results may be due to the fact that at lower concentrations of the added particles (here HAp and S45P7 BAG), the reinforcement particles in lesser number are unevenly distributed and are the reason for this lower strength, also the reinforcement particles may not be sufficient to uniformly prevent the dislocations movements in the strained matrix and hence provides lower strength. The strength of the composites was mainly due to two intervening phenomenon i.e. of grain refinement and dislocation of the grain boundary, and the porosity effect which tends to deteriorate the strength of the composites after a certain threshold. At higher concentrations (20 % HAp or S45P7 BAG or 10% HAp & 10 % S45P7 BAG) the flexural strength, hardness and compressive strength decreased, the reason of the decrease in strength may be due to the fact that there may be agglomeration of

reinforcement particles which causes poor interaction between the matrix and the foreign particle, also the porosity effect dominates at higher concentrations.

5.4 Summary of the chapter

The present chapter is focused on the study of physical, mechanical, and corrosion properties of the newly developed composite. It studied the effect of addition of HAp and S45P7 BAG particles in different proportions in the magnesium-zinc-manganese alloy matrix. The chapter studied and characterized the corrosion products formed on the composite surface after immersion in corrosive media. The concluding remarks of work done are as follows:

1. It can be concluded that with the increase in amount of HAp and S45P7 BAG, the bioactivity of the samples increased continuously. The FTIR data shows that the development of phosphate and carbonated bands on the surface of the samples after soaking in SBF solution occurred. It can be concluded that the more bioactivity was observed with 10% S45P7 BAG and 10% HAp composites compared to the lower percentage as well as pure alloys and individual metal–ceramic composites.
2. It was observed from the results that with increasing time, the apatite layer increases and covers more area on the surface, as shown in SEM micrographs, indicating better bioactivity of samples. It was found that globular apatite particles were deposited on the sample and more globular apatite was deposited after 2 weeks of immersion. HAp was formed only if the material is bio-active when immersed in SBF, it acted as a protection layer over its surface, thus increasing the corrosion resistance in physiological medium.
3. The mechanical characteristics of the different composites shows that at lower

concentration of the reinforcement, the strength is lower, it is maximum at 10 % of S45P7 BAG or HAp or both, and it again deteriorate at 20 %. It was due to the effect that at lower concentration, the matrix has not achieved optimized strength, and at higher percentage porosity and agglomeration of reinforcement have reduced the mechanical characteristics.